European Journal of Pediatrics (2024) 183:1183–1193
https://doi.org/10.1007/s00431-023-05363-9

RESEARCH

Normative computed tomography angiography values of the main and branch pulmonary arteries in children

Rakesh Donthula[1] · Wen Li[2,3] · Harmanpreet Kaur[1] · Dilachew A. Adebo[1] · Santosh C. Uppu[1]

Received: 4 October 2023 / Revised: 17 November 2023 / Accepted: 30 November 2023 / Published online: 11 December 2023

Abstract

Non-invasive cardiac imaging like echocardiogram, cardiac magnetic resonance imaging (CMR), and computed tomography angiography (CTA) play a key role in the diagnosis, aid in management and follow-up of congenital heart disease patients. Normative data for intracardiac and extracardiac vascular structures in children are currently available for echocardiogram, CMR, and non-gated CTA. We sought to establish systolic and diastolic normative data for main and branch pulmonary arteries in children using electrocardiogram (ECG)-gated CTA. Diameters and cross-sectional areas of the main and branch pulmonary arteries were measured in systole and diastole based on the aortic valve position (open versus closed) in 100 subjects who had ECG-gated cardiac CTA at our center between January 2015 through December 2020 and met our inclusion criteria. The allometric exponent (AE) for each parameter was derived, and the parameter/body surface area (BSA^{AE}) was established using the previously described methods. A total of 100 children aged 0–18 years were analyzed; mean age was 5.3 years (SD, 6.1 years). Z-score curves were plotted in relation to the BSA for the mean, maximum, and minimum diameters and cross-sectional area of the main and branch pulmonary arteries for systole and diastole.

Conclusion: We report systolic and diastolic mean, maximum, and minimum diameters and cross-sectional areas along with Z-scores and normative curves for the main and branch pulmonary arteries in children derived using ECG-gated cardiac CTA. We believe our results can help identify abnormally sized main and branch pulmonary arteries.

What is Known:
- *Normative data for intracardiac and extracardiac vascular structures in the pediatric population are available for echocardiography, cardiac MRI and non-ECG gated CTA.*
- *Z-scores with standard deviations are commonly used in children, but SDs are not constant across body sizes due to heteroscedasticity.*

What is New:
- *Allometric exponent was derived for each parameter and the parameter/body surface area (BSA) was established.*
- *This is the first ECG-gated CTA study to provide normative en face systolic, diastolic diameters and cross-sectional areas along with Z-scores and normative curves for the main and branch pulmonary arteries in children.*

Keywords Computed tomography angiography · Z-scores · Normative values · Pediatrics · Pulmonary artery

Communicated by Peter de Winter

✉ Santosh C. Uppu
uppusantosh@gmail.com

[1] The University of Texas Health Science Center at Houston, Children's Memorial Hermann Hospital, Houston, TX 77030, USA

[2] Division of Clinical and Translational Sciences, Department of Internal Medicine, the University of Texas McGovern Medical School at Houston, Houston, TX 77030, USA

[3] Biostatistics/Epidemiology/Research Design (BERD) Component, Center for Clinical and Translational Sciences (CCTS), The University of Texas Health Science Center at Houston, Houston, TX 77030, USA

Introduction

Significant advances in the diagnosis, management, and treatment of patients with congenital heart disease improved overall survival and outcomes [1, 2]. Non-invasive cardiac imaging like echocardiography (echo), cardiac gated computed tomography angiography (CTA), and cardiac magnetic resonance imaging (CMR) play a vital role in the diagnosis and follow-up of these patients [3–7]. Main and branch pulmonary arteries are commonly involved in patients with congenital heart defects. Normative data for intracardiac and extracardiac vascular structures in the pediatric population

are available for echo CMR and non-ECG gated CTA [8–12]. Previous attempts were made to derive Z-scores using non-ECG-gated CTA either using single planar or double-oblique measurement techniques [10–12].

Due to the lack of reliable Z-scores for ECG-gated CTA, imagers have difficulty interpreting these measurements and compensate it with known echo or CMR normative data [13, 14], which is not ideal due to the inherent variation of the imaging modalities.

The utility of CTA is gradually increasing and gaining acceptance in the congenital cardiology with improvements in scanning techniques, advances in radiation reduction, ease of access, and its ability to limit anesthesia exposure in young children due to fast scan times [6, 15]. Cross-sectional imaging with CTA and CMR has added benefit in advanced planning for interventional procedures, creation of virtual or 3D models, overlaying with angiography to reduce radiation dose of the intervention, etc. [16–19]. En face measurements using cross-sectional imaging are made to report major and minor dimensions for a structure as this negates the assumption that a vascular structure has a circular profile [11, 20].

Somatic growth should be considered for the pediatric population. For that reason, Z-scores are commonly used with standard deviations (SD) above and below a given measurement, but SDs are not constant across body sizes due to heteroscedasticity adding further complexity to the interpretation [21]. In this study, we sought to establish systolic and diastolic normative values and Z-scores for main and branch pulmonary arteries in children using ECG-gated CTA.

Methods

Data sources

The study was approved by the Institutional Review Board (HSC-MS-20–1338, September 13, 2021) and waived the need for informed consent. We conducted a retrospective chart review including all consecutive patients less than 21 years of age who underwent ECG-gated cardiac CTA between January 2015 and December 2020. We identified subjects using our imaging database and electronic medical records. Inpatient and outpatient records were analyzed to obtain baseline information.

Population

All children less than or equal to 21 years of age who underwent ECG-gated CTA were identified. Those subjects who met our inclusion criteria as listed in Table 1 were included in the final analysis. The diagnosis and indication of the CTA for the included subjects are listed in Table 2. We decided to include vascular ring subjects without intracardiac defects or genetic diagnosis in this study; these subjects are assumed to be "normal" for this study, as the main and branch pulmonary artery measurements are not affected by this diagnosis. This assumption may not be necessarily true, but it is not ethically possible to enroll normal subjects to undergo a CTA in order to derive Z-scores. As such, the number of subjects has been significantly lower compared to an echo study with similar goals.

Protocol for CTA

All patients were referred to our imaging center by a pediatric cardiologist. All referrals were screened by an attending imaging cardiologist prior to the cardiac CTA. All CTAs were performed using our institutional imaging protocol. Subjects younger than 6 weeks often underwent feed and swaddle technique to minimize the need for sedation. The need for sedation/anesthesia for subjects between 6 weeks and 6 years was individualized based on the imaging goal. Subjects less than 6 years requiring coronary artery evaluation were often anesthetized and intubated for better heart rate and respiratory control to avoid motion artifacts [22]. The location of the peripheral intravenous (PIV) access was determined by the imaging question. To evaluate for the aortic arch abnormalities, a foot PIV was preferred for contrast

Table 1 Inclusion and exclusion criteria

Inclusion criteria	Exclusion criteria
• Age ≤ 21 years of age	• Any CHD other than listed in the inclusion criteria
• Structurally normal heart	• Depressed ventricular function by echocardiogram
• Vascular ring	• Dilated cardiac chambers by echocardiogram
• Anomalous aortic origin of the coronary artery	• Genetic diagnosis
• Small patent ductus arteriosus in age < 1 month	• Motor vehicle accident with involvement to the heart
• Small patent foramen ovale	• Motion artifact
	• Post-operative CTA

CHD congenital heart defect

Table 2 Diagnosis of the included subjects

Diagnosis	Number (total $N = 100$)
Double aortic arch	13
Right aortic arch with aberrant left subclavian artery	25
Structurally normal heart	29
Anomalous Aortic origin of coronary arteries	RCA (16), LCA (3)
High origin of coronary artery above sinotubular junction	2
Kawasaki disease follow-up with no coronary involvement, normal ventricular function	3
Others	9

* *RCA* anomalous aortic origin of the right coronary artery, *LCA* anomalous aortic origin of the left coronary artery

injection. Iso-osmolar, nonionic, and water-soluble agent (Iodixanol, Visipaque™ 320 mg iodine/ml) was used for all the examinations [23]. The total contrast dose was 1.5–2 ml/kg of body weight. The contrast medium was administered using a dual-head power injector at an injection rate of 0.8–1.2 ml/s for a 24G PIV. The injection rate was increased based on the size of the PIV up to 4–5 ml/s [15, 24]. A bolus of isotonic saline solution was administered after contrast to reduce high-density contrast (streak) artifact. Automated bolus tracking technique was used with reference cardiovascular structure being monitored at near real-time until predetermined threshold opacification of 120–150 Hounsfield units was achieved at reference level. A scan delay of 4–5 s was often used for image acquisition [25].

Cardiac CTA technique

During the study period, different generations of Siemens CT scanners were used to perform these studies. These include SOMATOM AS 128, SOMATOM definition edge, and SOMATOM Force Dual-source CT (Siemens Healthineers AG©). Studies were performed according to our institutional protocol using a tube voltage of 70–100 kV, tube current auto modulation (CareDose4D, Siemens Healthineers AG©), and a slice thickness of 0.6 mm [24, 26, 27]. Retrospective ECG-gated acquisition was performed when ventricular volume/function and coronary artery evaluation were needed. The prospective ECG-triggered technique was used to delineate vascular anatomy [9]. Images were reconstructed with a slice thickness of 0.6 mm and an increment of 0.6 mm [28].

Images acquired when the aortic valve was open were included under systole; these were usually between 30 and 40% RR interval, and the images acquired when the aortic valve was closed were included under diastole, usually during 70–80% RR interval. Subjects who underwent retrospectively gated CTA had both systolic and diastolic images. Prospectively gated CTA images were acquired either in systole or diastole based on the subject's heart rate as per the machine algorithm and imager preference to minimize motion artifact. All studies were performed with an imaging cardiologist present during the scan.

Image post-processing

All measurements were performed on a cardiovascular imaging workstation (Circle CVI42; Circle Cardiovascular Imaging Inc. Alberta, Canada) after studies were anonymized. All images were visualized in axial, sagittal, and coronal planes with a window (600–900) and a level (250–350) settings. Double-oblique planes were obtained using multiplanar reformatting to measure MPA midway between the pulmonary valve and PA bifurcation. The proximal branch PAs were measured immediately after the PA bifurcation, all measures were made en face [20, 29]. Maximum, minimum, and mean diameters and cross-sectional area for MPA and branch PAs by planimetry were measured (Fig. 1). The measurements were categorized as either systolic or diastolic as described above.

Statistical analysis

Data was expressed as mean ± SD. The measure of the vessel was indexed to the body surface area (BSA) according to the Haycock formula [30]. The allometric exponent for each parameter was derived by applying the ordinary least squares method in which the natural logarithm of the parameter was regressed on the natural logarithm of BSA [31]. This method allows for a nonlinear relationship between the parameter and BSA. Specifically, the following steps were used.

1. The equation $Y = mX^b$ was considered to decide the potentially nonlinear relationship between a parameter and BSA. Y denoted the parameter, X denoted BSA, and b was the AE to be estimated.
2. After taking natural log, a linear regression formula was obtained: $lnln(Y) = lnln(m) + blnln(X)$,, where

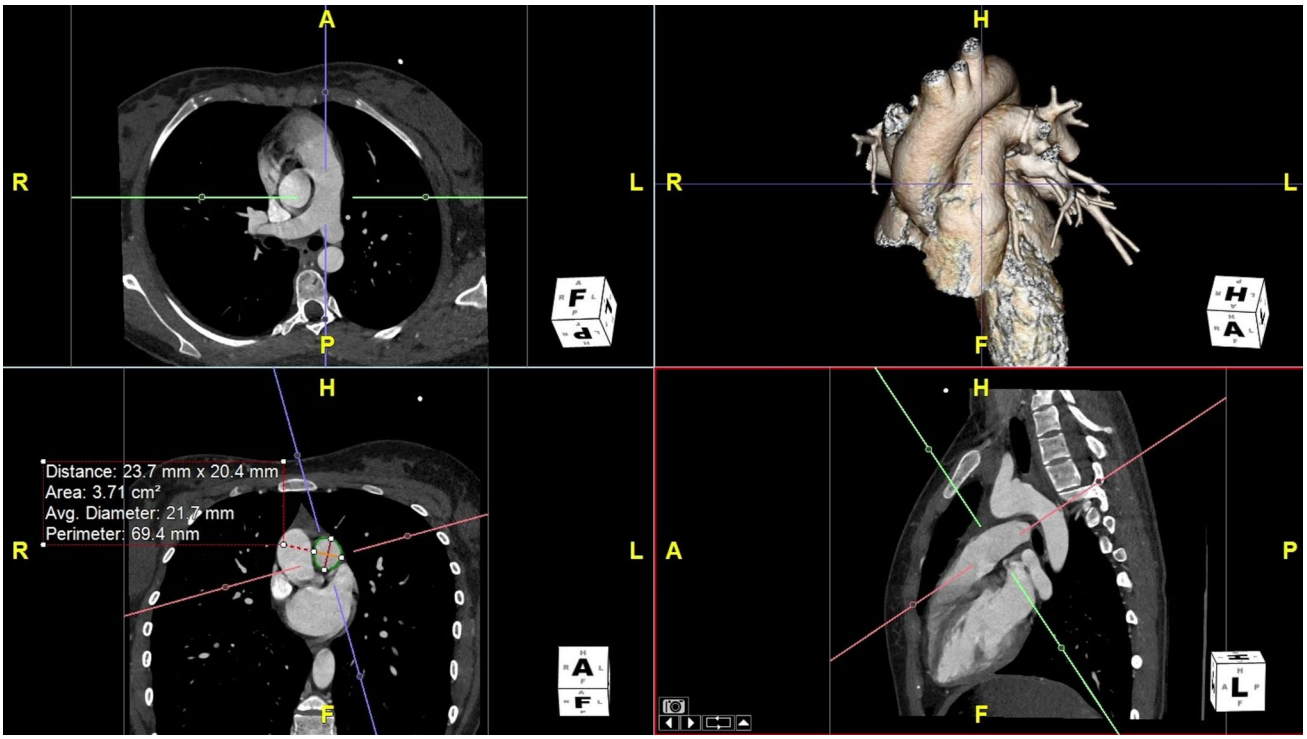

Fig. 1 Example obtaining a double oblique plane using multiplanar reformatting of the main pulmonary artery to measure maximum, minimum, and mean diameters and cross-sectional area

ln(Y) was the dependent variable and ln(X) was the independent variable.

3. The regression coefficient estimate $\widehat{b}$ for b from the least s draft was condensed squares model was the derived AE.

We then indexed the parameter using BSA to the power of the derived AE. We did the following quality check to make sure that the allometric model was adequate and that there was no residual relationship between the indexed parameter and BSA. The indexed parameter was regressed against BSA. The regression line was plotted, and R^2 was calculated. A flat line and a small R^2 indicate no residual relationship. Pearson correlation coefficient and the corresponding P value were determined. A correlation close to zero and a P-value ≥ 0.05 also indicate no residual relationship.

We checked the normality of the indexed parameter using the Shapiro–Wilk test and reported $\mu \pm \sigma$ where μ and σ denoted the mean and SD of the indexed parameter. Last, we derived Z-scores for the nonindexed parameter by BSA based on the relationship that the nonindexed parameter followed a normal distribution with a mean of $\mu \mathrm{BSA}^{\mathrm{AE}}$ and SD of σ $\mathrm{BSA}^{\mathrm{AE}}$.

Interobserver and intraobserver variability were assessed using the intraclass correlation coefficient in a subset of 50 subjects. All analyses were conducted using R version 4.0.5 (March 2021).

Results

Patient characteristics

Out of 628 patients who underwent CTA at our institution during the study period, 100 children met the inclusion criteria and were analyzed. The mean age and BSA of the subjects were 5.3 ± 6.1 years (range 0–18) and 0.8 ± 0.68 m^2 (range 0.16–2.8), respectively. Among the subjects, 56% were male (Table 3). The majority (71%) of our subjects were young with a BSA < 1 m^2. The most common finding on the CTA was a vascular ring ($n = 38$), followed by structurally normal heart ($n = 29$), and coronary anomaly ($n = 21$) as shown in Table 2. Systolic measurements were available for most of

Table 3 Demographics and baseline characteristics

Sex (%)	Male (56%)	
BSA < 1 m^2	71%	
	Mean (SD)	**Median (range)**
Age	5.3 years (6.1)	2.3 years (0–18)
Weight	26.2 kg (31.4)	12.75 kg (2.04–156)
Height	98 cm (47.8)	88.5 cm (44–187)
BSA	0.8 m^2 (0.68)	0.6 m^2 (0.16–2.8)

BSA body surface area, *SD* standard deviation

our subjects (RPA, $n=87$; LPA, $n=89$; and MPA, $n=92$, respectively), and diastolic measurements were available for 45 subjects. This is due to the younger age of our study population; the CTA imaging protocols are geared towards acquiring the image during the least heart motion to reduce artifacts. As such, systolic imaging is common in young children due to fast heart rates.

Normative values

The normalized mean, maximum, and minimum diameters (mm), cross-sectional area (mm^2), and standard deviation of the MPA and branch PAs for systole and diastole are shown in Tables 4 and 5.

The Z-score plots for mean systolic and diastolic diameters and cross-sectional areas of MPA, RPA, and LPA are shown in Figs. 2 and 3. The Z-score plots for the maximum and minimum diameters are shown in Figs. 4 and 5.

As expected, systolic diameters were 9–12% larger, and systolic cross-sectional areas were 18–20% larger compared to diastolic measures. As previously observed, main and branch PAs were not perfectly circular in our study with maximum diameters at least 1–2 mm larger than the minimum diameters.

Reproducibility

There was an excellent inter and intraobserver agreement (> 0.94) for both systolic and diastolic measurements for all the measurements (Tables 6 and 7) indicating excellent reproducibility of our technique.

Table 4 Maximum, minimum, mean, area variables with AE, SD in systole

Systolic parameter	*N*	AE	Mean	Standard deviation
LPA Max	89	0.65	14.352	2.454
LPA Min	89	0.66	12.791	2.288
LPA Mean	89	0.66	13.571	2.308
LPA area	89	1.32	148.084	47.974
MPA Max	92	0.49	20.282	2.604
MPA Min	92	0.49	18.511	2.5
MPA Mean	92	0.49	19.397	2.444
MPA area	92	0.98	299.07	74.127
RPA Max	87	0.62	14.667	2.556
RPA Min	87	0.62	12.283	2.617
RPA Mean	87	0.62	13.451	2.428
RPA area	87	1.25	145.52	52.008

LPA left pulmonary artery, *RPA* right pulmonary artery, *MPA* main pulmonary artery, *Max* maximum diameter, *Min* minimum diameter, *Mean* mean diameter, *area* cross-sectional area, *N* number of subjects, *AE* allometric exponent, *SD* standard deviation

Max, min, and mean diameters are reported in millimeters, and cross-sectional area is reported in square millimeters. Systolic measurements were available for RPA in 87, LPA in 89, and MPA in 92 subjects, respectively

Table 5 Maximum, minimum, mean, area variables with AE, SD in diastole

Diastolic parameter	*N*	AE	Mean	Standard deviation
LPA Max	45	0.57	13.125	2.312
LPA Min	45	0.6	11.302	2.205
LPA Mean	45	0.58	12.212	2.132
LPA area	45	1.17	119.574	41.938
MPA Max	45	0.52	18.137	2.433
MPA Min	45	0.51	16.188	2.164
MPA Mean	45	0.52	17.163	2.208
MPA area	45	1.03	234	60.72
RPA Max	45	0.55	13.323	2.304
RPA Min	45	0.55	11.101	2.065
RPA Mean	45	0.55	12.21	2.089
RPA area	45	1.1	119.187	41.223

LPA left pulmonary artery, *RPA* right pulmonary artery, *MPA* main pulmonary artery, *Max* maximum diameter, *Min* minimum diameter, *Mean* mean diameter, *area* cross-sectional area, *N* number of subjects, *AE* allometric exponent, *SD* standard deviation

Max, min, and mean diameters are reported in millimeters, and cross-sectional area is reported in square millimeters. Diastolic measurements were available in 45 subjects

Discussion

Our study provides normative systolic and diastolic diameters and cross-sectional areas along with Z-scores and normative curves for the main and branch pulmonary arteries in children derived using ECG-gated cardiac CTA. We report maximum, minimum, and mean diameters as well as the cross-sectional area for these structures. Normative values in children exist for echo, CMR, and non-ECG-gated CTA [13, 14, 33–35]. Few non-ECG-gated CTA studies reported normative measurements of main and branch PAs. Akay et al. [12] and Bayindir et al. [10] used single measurements from standard axial imaging planes in their studies. These measurements did not take the patient size into account; as such, the influence of growth and body size in a patient cannot be assessed. This methodology can also be challenging especially in patients with congenital heart defects, heterotaxy, etc. where a single-plane measurement may not be practical. Greenberg et al. [11] did a good attempt at reporting pulmonary artery measurement using the double-oblique method using chest CTAs performed mostly in oncology patients; their measurement technique was similar to our study. However, they have not used ECG-gated CTAs which the authors have recognized as a limitation. Their data was modeled using a natural log-transformed response variable

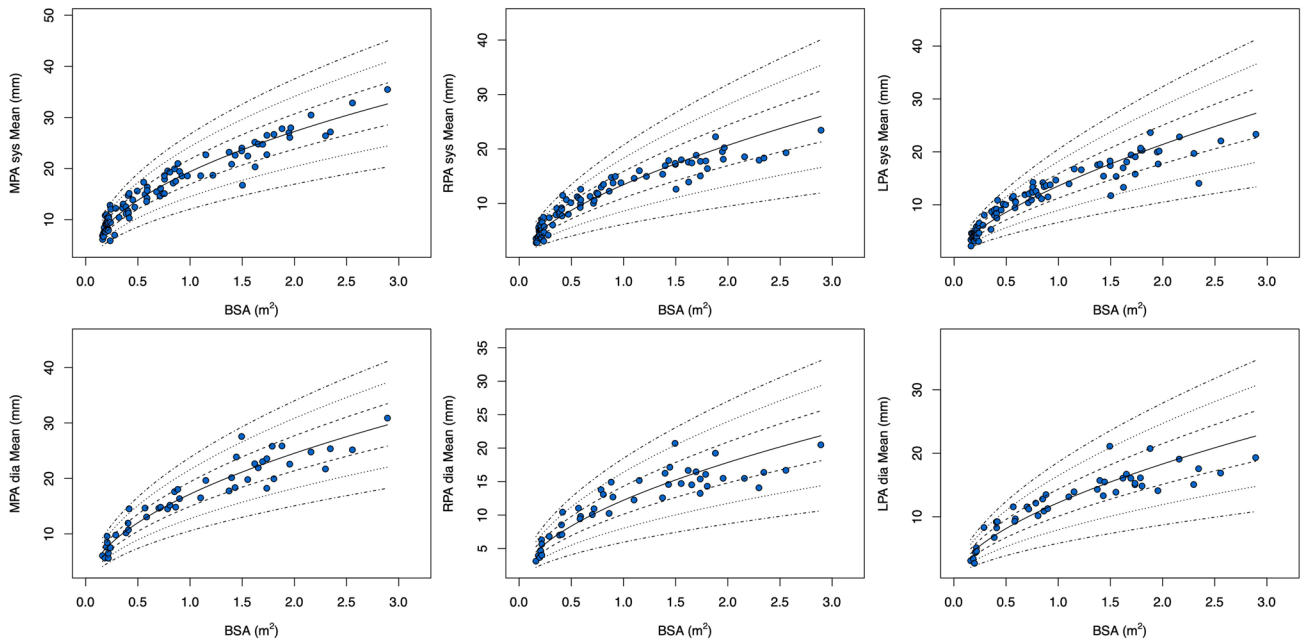

Fig. 2 Regression lines for Z-score plots between − 3.0 and + 3.0 for indexed MPA, RPA, and LPA mean diameters in systole and diastole. MPA main pulmonary artery, RPA right pulmonary artery, LPA left pulmonary artery, Sys systole, Dia diastole

and a linear term for height as the independent variable. In contrast, we have used the allometric exponent for each parameter and the parameter/body surface area (BSA^{AE}). This methodology has wider acceptance in the congenital cardiology and is widely used for echo Z-score calculations. They also noticed that the pulmonary arteries are oval in > 50% similar to our results.

En face measurements of the main and branch PAs provide an accurate assessment of the structure and negate the assumption that vascular structures have a circular profile

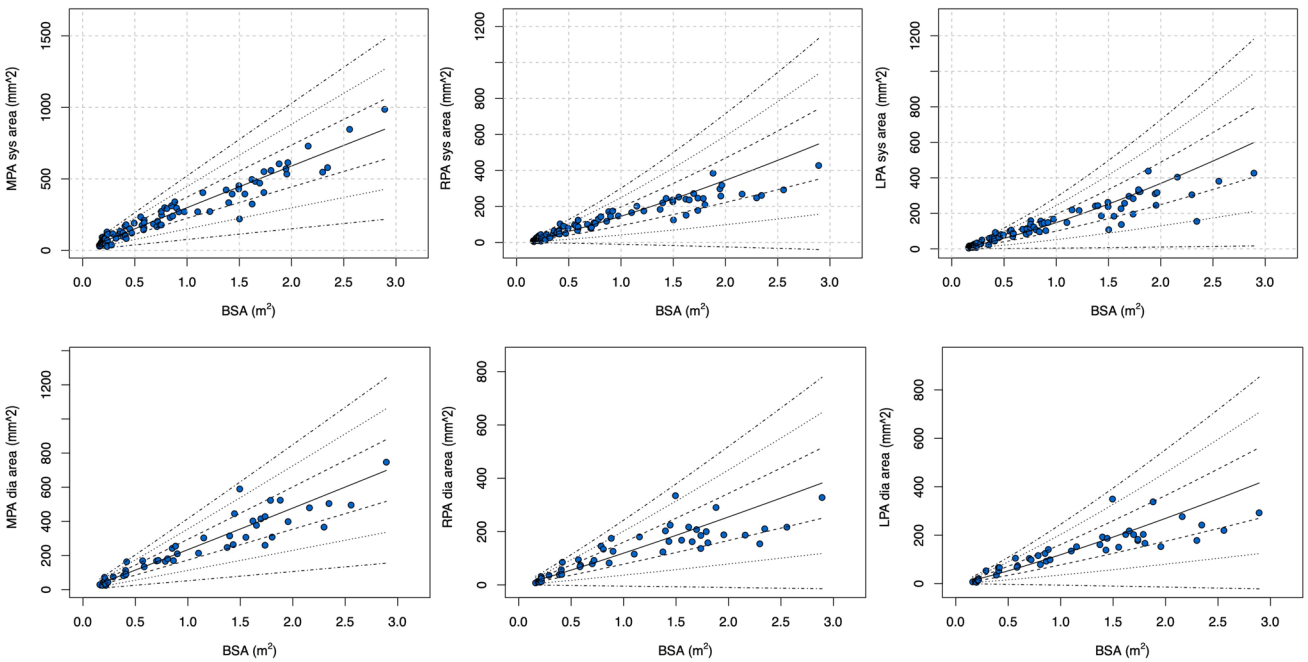

Fig. 3 Regression lines for Z-score plots between − 3.0 and + 3.0 for indexed MPA, RPA, and LPA cross-sectional areas in systole and diastole. MPA main pulmonary artery, RPA right pulmonary artery, LPA left pulmonary artery, Sys systole, Dia diastole

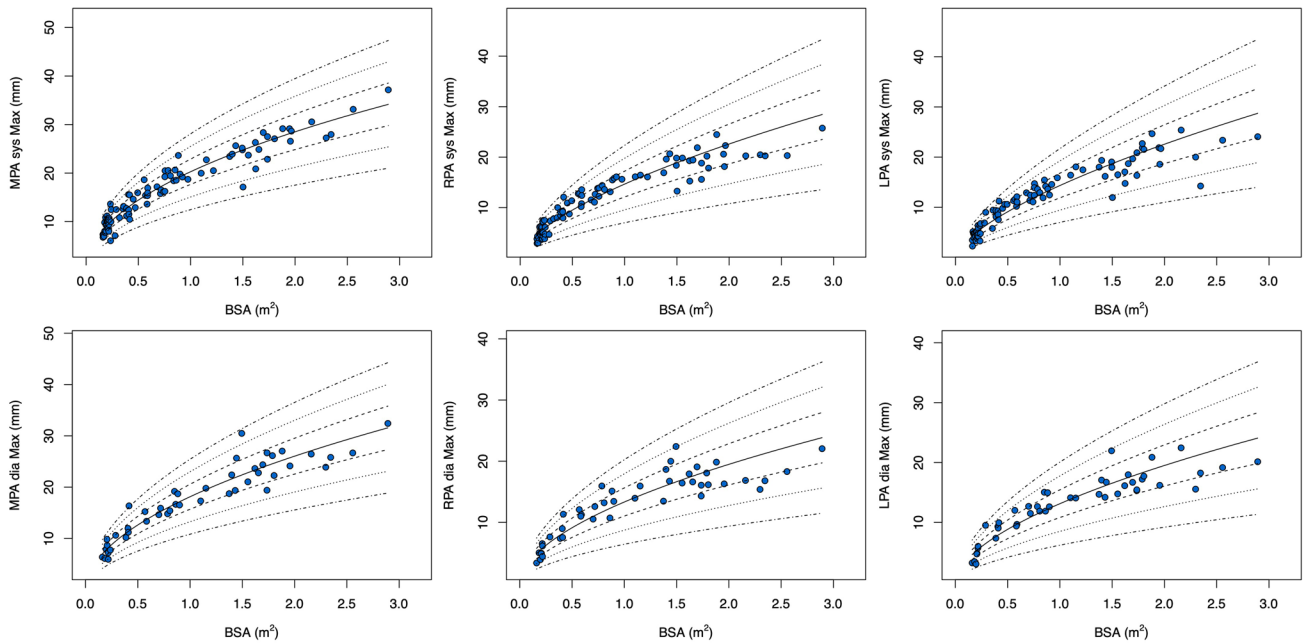

Fig. 4 Regression lines for Z-score plots between − 3.0 and + 3.0 for indexed MPA, RPA, and LPA maximum diameters in systole and diastole. MPA main pulmonary artery, RPA right pulmonary artery, LPA left pulmonary artery, Sys systole, Dia diastole

[20]. Pulmonary arteries are commonly involved in patients with congenital heart defects; as such, better understanding is necessary for appropriate planning, risk stratification, and management. Cardiac ECG-gated CTA is gaining acceptance in congenital cardiology to better evaluate vascular structures due to the improvements of scanning techniques, radiation reduction, ease of access, fast scan times, and reduced need for anesthesia in young children [6, 26]. To our knowledge, this is the first cardiac ECG-gated study to report normative data for the main and branch PAs.

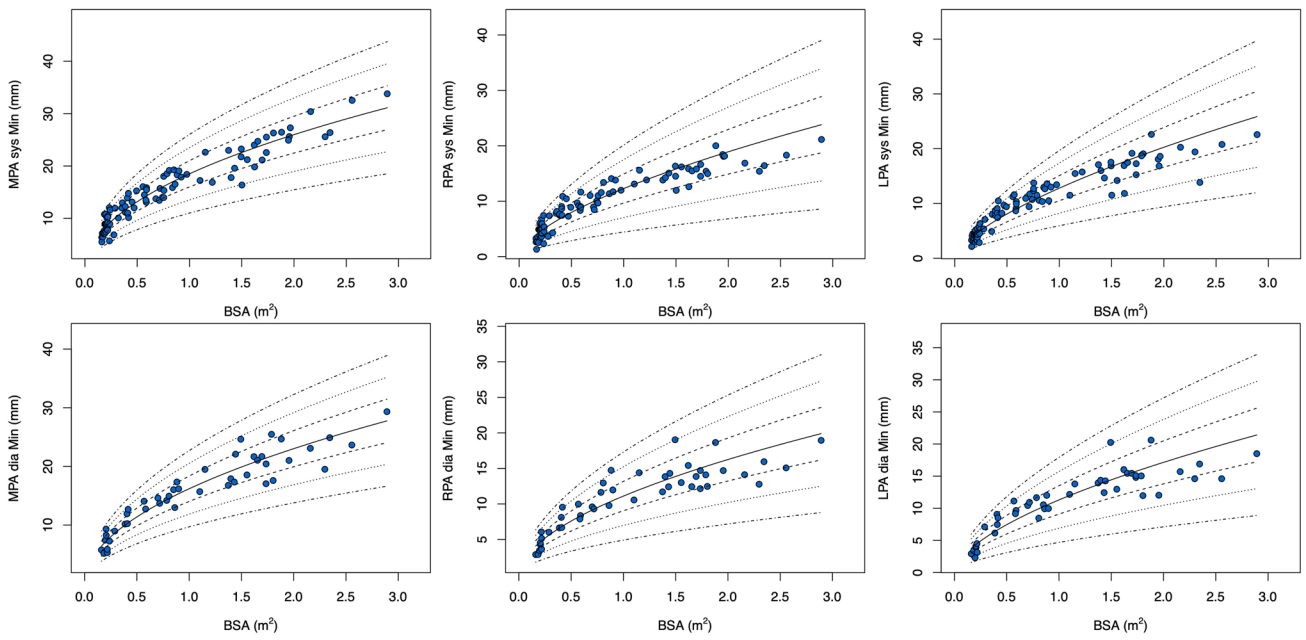

Fig. 5 Regression lines for Z-score plots between − 3.0 and + 3.0 for indexed MPA, RPA, and LPA minimum diameters in systole and diastole. MPA main pulmonary artery, RPA right pulmonary artery, LPA left pulmonary artery, Sys systole, Dia diastole

Table 6 Inter and intraobserver variables in systole

Systolic parameter	Intra-rater	95% CI	Inter-rater	95% CI
LPA Max	0.992	(0.981, 0.997)	0.983	(0.954, 0.994)
LPA Min	0.975	(0.938, 0.99)	0.976	(0.935, 0.992)
LPA Mean	0.987	(0.968, 0.995)	0.982	(0.95, 0.994)
MPA Max	0.982	(0.955, 0.993)	0.979	(0.938, 0.993)
MPA Min	0.964	(0.91, 0.986)	0.961	(0.887, 0.987)
MPA Mean	0.98	(0.951, 0.992)	0.976	(0.928, 0.992)
RPA Max	0.972	(0.931, 0.989)	0.978	(0.94, 0.992)
RPA Min	0.98	(0.951, 0.992)	0.975	(0.931, 0.991)
RPA Mean	0.981	(0.952, 0.992)	0.98	(0.945, 0.993)

LPA left pulmonary artery, *RPA* right pulmonary artery, *MPA* main pulmonary artery, *Max* maximum diameter, *Min* minimum diameter, *Mean* mean diameter, *CI* confidence interval

Our study is also unique in reporting both systolic and diastolic normative values, and our study confirms larger systolic parameters compared with diastolic measures as was previously described by an angiographic study [36].

Cross-sectional area along with mean diameter may have real-world applicability as the structure of interest can be assessed in any non-standard plane. This is especially important in patients with congenital heart defects where a vascular structure may not be in a normal orientation as in crossing or supero-inferior branch PAs, dextrocardia, etc.

Deriving normative values and Z-scores can be achieved by various methods, and there is significant variation among Z-scores derived from each method [37–40]. We chose the previously described and validated method of using BSA as an expression of body size and linear regression for the relationship between body growth and cardiovascular dimensions [21, 31, 33, 41–43]. Cardiovascular allometry is defined as the relative growth of cardiac structure in relation to somatic growth. Identifying a correct allometric relationship and model for a structure is important for its interpretation and clinical application [32, 41]. Multiple authors have advocated the use of an allometric model to identify a true indexing method of a physiologically dependent variable, and this method has been widely used for various echo Z-score calculators that are in current clinical use [31–33, 41, 42].

Our study population was mostly young with 71% having a BSA less than 1 m^2; subjects with complex congenital heart defects tend to get cross-sectional imaging around the perioperative/peri-interventional period, especially when they are young. As such, we believe our normative values and Z-scores will help this population with appropriate planning.

Recruiting normal children for a CTA study is ethically challenging due to radiation exposure, the need for sedation/anesthesia, and contrast administration. It is not uncommon to identify normal subjects who undergo cross-sectional imaging for various reasons to be included in a study. Prior CMR studies from 2008 and 2011 included children with a history of malignancy to derive normative values for aorta and pulmonary arteries [13, 14]. We have been diligent to include subjects with normal pulmonary arterial anatomy; as a result, this data should be close to what is expected for a normal population. Future studies are needed to validate our results with a larger sample. We plan to make our data publicly available.

Table 7 Inter and intraobserver variables in diastole

Diastolic parameter	Intra-rater	95% CI	Inter-rater	95% CI
LPA Max	0.953	(0.832, 0.988)	0.942	(0.798, 0.985)
LPA Min	0.969	(0.887, 0.992)	0.968	(0.885, 0.992)
LPA Mean	0.973	(0.903, 0.993)	0.973	(0.901, 0.993)
MPA Max	0.952	(0.799, 0.99)	0.964	(0.86, 0.992)
MPA Min	0.972	(0.879, 0.994)	0.966	(0.867, 0.992)
MPA Mean	0.982	(0.921, 0.996)	0.975	(0.9, 0.994)
RPA Max	0.986	(0.95, 0.996)	0.965	(0.873, 0.991)
RPA Min	0.988	(0.957, 0.997)	0.992	(0.969, 0.998)
RPA Mean	0.993	(0.976, 0.998)	0.986	(0.949, 0.997)

LPA left pulmonary artery, *RPA* right pulmonary artery, *MPA* main pulmonary artery, *Max* maximum diameter, *Min* minimum diameter, *Mean* mean diameter, *CI* confidence interval

Limitations

Our single-center, small-sample, retrospective study has inherent limitations due to its design. Generalized applicability across institutions may not be possible, but there is a lack of normative ECG-gated CTA data available at this time. Our data will help kick-start the process of performing a similar study in a multicenter fashion which can help address issues related to a single-center design. Similar goals have been achieved by the Pediatric Heart Network echocardiogram database that published echocardiographic Z-scores recently, although normative echo Z-scores have been in existence for a few decades. The statistical methodology may have issues with the model of choice; there has been extensive literature on various Z-score models, but we felt that our approach is ideal for this study based on extensive prior experience using allometric models in echocardiographic Z-score studies. It would have been interesting to compare our CT-derived Z-scores with the existing echo and CMR Z-scores, but it is not feasible to make a meaningful comparison as these methods employ different measurement and imaging techniques. Our study has not explored the influence of sex or race on the Z-scores due to the small sample size; a multicenter design is likely to address this issue. Our sample has predominantly young children; its applicability for older children and adolescents should be done with caution.

Conclusions

This is the first study to report en face normative diameters and cross-sectional areas of main and branch pulmonary arteries in systole and diastole derived using gated cardiac CTA. This data has potential application for proper diagnosis, risk stratification, and planning for surgical and catheter-related interventions for children with congenital heart defects. The real-world applicability of this tool needs careful validation.

Authors' contributions All authors contributed to the study conception and design. Material preparation, data collection, and analysis were performed by Harmanpreet Kaur, Rakesh Donthula, and Santosh Uppu. Statistical analysis was performed by Wen Li. The first draft of the manuscript was written by Rakesh Donthula and Santosh Uppu. All authors commented on previous versions of the manuscript. All authors read and approved the final manuscript. We would also like to acknowledge the contribution of Dan Dyar, MA, RDCS, FASE from Rady Children's hospital, San Diego in the addendum who checked our published tables and Figures and recommended the correction of these Figures.

Funding Dr. Wen Li's effort is supported by UL1TR003167. The other authors declare that no funds, grants, or other support were received during the preparation of this manuscript.

Data availability The anonymized data used for this study are available from the corresponding author upon reasonable request.

Declarations

Competing interests The authors declare no competing interests.

Conference presentation Abstract was presented at the North American Society of Cardiovascular Imaging (NASCI) conference in Cleveland, OH on September 11 2022.

Ethical approval This study was approved by The University of Texas Health Science Center at Houston and Memorial Hermann Institutional Review Board (HSC-MS-20–1338, September 13, 2021) and waived the need for informed consent. All human studies at the University of Texas at Houston Health Science Center and Memorial Hermann hospital have to go through rigorous review by the ethics committee and have therefore been performed in accordance with the ethical standards laid down in the 1964 Declaration of Helsinki and its later amendments. The subjects were deidentified as per our IRB guidelines. Due to the retrospective nature, this study does not require contacting subjects, as such a waiver of consent was requested and was approved by the IRB.

References

1. Marelli AJ, Ionescu-Ittu R, Mackie AS, Guo L, Dendukuri N, Kaouache M (2014) Lifetime prevalence of congenital heart disease in the general population from 2000 to 2010. Circulation 130(9):749–756. https://doi.org/10.1161/CIRCULATIONAHA.113.008396
2. Gilboa SM, Devine OJ, Kucik JE et al (2016) Congenital heart defects in the united states: estimating the magnitude of the affected population in 2010. Circulation 134(2):101–109. https://doi.org/10.1161/CIRCULATIONAHA.115.019307
3. Prakash A, Powell AJ, Geva T (2010) Multimodality noninvasive imaging for assessment of congenital heart disease. Circ Cardiovasc Imaging 3(1):112–125. https://doi.org/10.1161/CIRCIMAGING.109.875021
4. Weber O, Higgins C (2006) MR evaluation of cardiovascular physiology in congenital heart disease: flow and function. J Cardiovasc Magn Reson 8(4):607–617. https://doi.org/10.1080/10976640600740254
5. Crean A (2007) Cardiovascular MR and CT in congenital heart disease. Heart 93(12):1637–1647. https://doi.org/10.1136/hrt.2006.104729
6. Han BK, Rigsby CK, Hlavacek A et al (2015) Computed tomography imaging in patients with congenital heart disease Part I: rationale and utility. An Expert Consensus Document of the Society of Cardiovascular Computed Tomography (SCCT): Endorsed by the Society of Pediatric Radiology (SPR) and the North American Society of Cardiac Imaging (NASCI). J Cardiovasc Comput Tomogr 9(6):475–492. https://doi.org/10.1016/j.jcct.2015.07.004
7. Fratz S, Chung T, Greil GF et al (2013) Guidelines and protocols for cardiovascular magnetic resonance in children and adults with congenital heart disease: SCMR expert consensus group on congenital heart disease. J Cardiovasc Magn Reson 15:51. https://doi.org/10.1186/1532-429X-15-51
8. Sarikouch S, Peters B, Gutberlet M et al (2010) Sex-specific pediatric percentiles for ventricular size and mass as reference values for cardiac MRI: assessment by steady-state free-precession and phase-contrast MRI flow. Circ Cardiovasc Imaging 3(1):65–76. https://doi.org/10.1161/CIRCIMAGING.109.859074

9. Achenbach S, Ulzheimer S, Baum U et al (2000) Noninvasive coronary angiography by retrospectively ECG-gated multislice spiral CT. Circulation 102(23):2823–2828. https://doi.org/10.1161/01.cir.102.23.2823
10. Bayindir P, Bayraktaroglu S, Ceylan N, Savas R, Alper HH (2016) Multidetector computed tomographic assessment of the normal diameters for the thoracic aorta and pulmonary arteries in infants and children. Acta Radiol 57(10):1261–1267. https://doi.org/10.1177/0284185115622074
11. Greenberg SB, Lang SM, Gauss CH, Lensing SY, Ali S, Lyons KA (2018) Normal pulmonary artery and branch pulmonary artery sizes in children. Int J Cardiovasc Imaging 34(6):967–974. https://doi.org/10.1007/s10554-018-1303-7
12. Akay HO, Ozmen CA, Bayrak AH et al (2009) Diameters of normal thoracic vascular structures in pediatric patients. Surg Radiol Anat 31(10):801–807. https://doi.org/10.1007/s00276-009-0525-8
13. Kaiser T, Kellenberger CJ, Albisetti M, Bergsträsser E, Valsangiacomo Buechel ER (2008) Normal values for aortic diameters in children and adolescents–assessment in vivo by contrast-enhanced CMR-angiography. J Cardiovasc Magn Reson 10:56. https://doi.org/10.1186/1532-429X-10-56
14. Knobel Z, Kellenberger CJ, Kaiser T, Albisetti M, Bergsträsser E, Buechel ERV (2011) Geometry and dimensions of the pulmonary artery bifurcation in children and adolescents: assessment in vivo by contrast-enhanced MR-angiography. Int J Cardiovasc Imaging 27(3):385–396. https://doi.org/10.1007/s10554-010-9672-6
15. Han BK, Rigsby CK, Leipsic J et al (2015) Computed tomography imaging in patients with congenital heart disease, Part 2: technical recommendations. An Expert Consensus Document of the Society of Cardiovascular Computed Tomography (SCCT): Endorsed by the Society of Pediatric Radiology (SPR) and the North American Society of Cardiac Imaging (NASCI). J Cardiovasc Comput Tomogr 9(6):493–513. https://doi.org/10.1016/j.jcct.2015.07.007
16. Farooqi KM, Nielsen JC, Uppu SC et al (2015) Use of 3-dimensional printing to demonstrate complex intracardiac relationships in double-outlet right ventricle for surgical planning. Circ Cardiovasc Imaging 8(5). https://doi.org/10.1161/CIRCIMAGING.114.003043
17. Farooqi KM, Uppu SC, Nguyen K et al (2016) Application of virtual three-dimensional models for simultaneous visualization of intracardiac anatomic relationships in double outlet right ventricle. Pediatr Cardiol 37(1):90–98. https://doi.org/10.1007/s00246-015-1244-z
18. Adebo DA, Uppu SC, Aggarwal A, Salazar JD, LaPar DJ (2022) Virtual simulated implantation of an adult-sized left ventricular assist device in a pediatric patient. JACC Case Rep 4(4):239–240. https://doi.org/10.1016/j.jaccas.2021.11.025
19. Arar Y, Reddy SRV, Kim H et al (2020) 3D advanced imaging overlay with rapid registration in CHD to reduce radiation and assist cardiac catheterisation interventions. Cardiol Young 30(5):656–662. https://doi.org/10.1017/S1047951120000712
20. Bradshaw KA, Pagano D, Bonser RS, McCafferty I, Guest PJ (1998) Multiplanar reformatting and three-dimensional reconstruction: for pre-operative assessment of the thoracic aorta by computed tomography. Clin Radiol 53(3):198–202. https://doi.org/10.1016/s0009-9260(98)80100-1
21. Colan SD (2013) The why and how of Z scores. J Am Soc Echocardiogr 26(1):38–40. https://doi.org/10.1016/j.echo.2012.11.005
22. Husmann L, Herzog BA, Pazhenkottil AP et al (2011) Lowering heart rate with an optimised breathing protocol for prospectively ECG-triggered CT coronary angiography. Br J Radiol 84(1005):790–795. https://doi.org/10.1259/bjr/29696915
23. Spencer CM, Goa KL (1996) Iodixanol. A review of its pharmacodynamic and pharmacokinetic properties and diagnostic use as an x-ray contrast medium. Drugs 52(6):899–927. https://doi.org/10.2165/00003495-199652060-00013
24. Uppu SC (2021) Left ventricular outflow tract. In: Adebo DA (ed) Pediatric Cardiac CT in Congenital Heart Disease Springer International Publishing. pp 107–113. https://doi.org/10.1007/978-3-030-74822-7_15
25. Adebo DA (2021) Techniques of cardiac CT scan: patient preparation, contrast medium, scanning, and post-processing. In: Adebo DA (ed) Pediatric Cardiac CT in Congenital Heart Disease Springer International Publishing. pp 15–22. https://doi.org/10.1007/978-3-030-74822-7_2
26. Dodge-Khatami J, Adebo DA (2021) Evaluation of complex congenital heart disease in infants using low dose cardiac computed tomography. Int J Cardiovasc Imaging 37(4):1455–1460. https://doi.org/10.1007/s10554-020-02118-7
27. Vasquez Choy AL, Adebo DA, John S, Greenleaf CE, Salazar JD, Corno AF (2022) Essential role of cardiac computed tomography for surgical decision making in children with total anomalous pulmonary venous connection and single ventricle. J Card Surg 37(6):1544–1549. https://doi.org/10.1111/jocs.16427
28. Alshipli M, Kabir NA (2017) Effect of slice thickness on image noise and diagnostic content of single-source-dual energy computed tomography. J Phys: Conf Ser 851:012005. https://doi.org/10.1088/1742-6596/851/1/012005
29. Bell D, Fortin F (2005) Multiplanar reformation (MPR). In: Radiopaedia.org. https://doi.org/10.53347/rID-65727
30. Nevill AM, Bate S, Holder RL (2005) Modeling physiological and anthropometric variables known to vary with body size and other confounding variables. Am J Phys Anthropol 41:141–153. https://doi.org/10.1002/ajpa.20356
31. Bhatla P, Nielsen JC, Ko HH, Doucette J, Lytrivi ID, Srivastava S (2012) Normal values of left atrial volume in pediatric age group using a validated allometric model. Circ Cardiovasc Imaging 5(6):791–796. https://doi.org/10.1161/CIRCIMAGING.112.974428
32. Rajagopal H, Uppu SC, Weigand J et al (2018) Validation of right atrial area as a measure of right atrial size and normal values of in healthy pediatric population by two-dimensional echocardiography. Pediatr Cardiol 39(5):892–901. https://doi.org/10.1007/s00246-018-1838-3
33. Lopez L, Colan S, Stylianou M et al (2017) Relationship of echocardiographic Z scores adjusted for body surface area to age, sex, race, and ethnicity: the pediatric heart network normal echocardiogram database. Circ Cardiovasc Imaging 10(11). https://doi.org/10.1161/CIRCIMAGING.117.006979
34. Lopez L, Frommelt PC, Colan SD et al (2021) Pediatric Heart Network echocardiographic Z scores: comparison with other published models. J Am Soc Echocardiogr 34(2):185–192. https://doi.org/10.1016/j.echo.2020.09.019
35. Voges I, Giordano R, Koestenberg M et al (2019) Nomograms for cardiovascular magnetic resonance measurements in the pediatric age group: to define the normal and the expected abnormal values in corrected/palliated congenital heart disease: a systematic review. J Magn Reson Imaging 49(5):1222–1235. https://doi.org/10.1002/jmri.26614
36. Rammos S, Kramer HH, Trampisch HJ, Krogmann ON, Kozlik R, Bourgeois M (1989) [Normal values of the growth of the pulmonary arteries in children. An angiography study]. Herz 14(6):348–357
37. Chubb H, Simpson JM (2012) The use of Z-scores in paediatric cardiology. Ann Pediatr Cardiol 5(2):179–184. https://doi.org/10.4103/0974-2069.99622
38. Pettersen MD, Du W, Skeens ME, Humes RA (2008) Regression equations for calculation of z scores of cardiac structures in a large cohort of healthy infants, children, and adolescents: an echocardiographic study. J Am Soc Echocardiogr 21(8):922–934. https://doi.org/10.1016/j.echo.2008.02.006

39. Zilberman MV, Khoury PR, Kimball RT (2005) Two-dimensional echocardiographic valve measurements in healthy children: gender-specific differences. Pediatr Cardiol 26(4):356–360. https://doi.org/10.1007/s00246-004-0736-z
40. Cantinotti M, Giordano R, Scalese M et al (2017) Nomograms for two-dimensional echocardiography derived valvular and arterial dimensions in Caucasian children. J Cardiol 69(1):208–215. https://doi.org/10.1016/j.jjcc.2016.03.010
41. Sluysmans T, Colan SD (2005) Theoretical and empirical derivation of cardiovascular allometric relationships in children. J Appl Physiol 99(2):445–457. https://doi.org/10.1152/japplphysiol.01144.2004
42. Colan SD (2016) Normal echocardiographic values for cardiovascular structures. In: Lai WW, Mertens LL, Cohen MS, Geva T (eds) Echocardiography in Pediatric and Congenital Heart Disease: From Fetus to Adult. John Wiley & Sons, Ltd. pp 883–901. https://doi.org/10.1002/9781118742440.app1
43. Sluysmans T, Colan SD (2009) Structural measurements and adjustment for growth. In: Lai WW, Mertens LL, Cohen MS, Geva T (eds) *Echocardiography in Pediatric and Congenital Heart Disease: From Fetus to Adult*. 1st ed. Wiley-Blackwell. pp 53–61